



COMPARISON OF EXPERIMENTAL CURVES OF ESP WITH A SIMPLE SINGLE-PHASE APPROACH

Jorge Luiz Biazussi
William Monte Verde
Maurício Pardo Varón
Antonio Carlos Bannwart

States University of Campinas – UNICAMP – Department of Petroleum Engineering – Campinas - SP
jorge.biazussi@gmail.com
williammonteverde@gmail.com
mapardo19@gmail.com
bannwart@fem.unicamp.br

Valdir Estevam

Petrobras – Av. Rep. Chile, 330 - 7º - Centro Rio de Janeiro - RJ
vestevam@petrobras.br

Abstract. *The utilization of an ESP (Electrical Submersible Pump) is one the most important artificial lift methods for petroleum production in Brazil and worldwide. The pressure gain provided by a bottom-hole multistage centrifugal pump adds to the reservoir pressure so as the fluid reaches the surface facilities at the desired flow rate. In this paper, a method to interpret the pump performance curves (head-capacity, power-capacity and efficiency capacity) is discussed. The method is based upon an algebraic representation of the pressure losses of the fluid passing through the pump. Similarly, power losses associated with the fluid surrounding the impeller are described. To validate the method, a three-stage pump was tested in laboratory using water and mineral oils of different viscosities. The algebraic correlations were fitted to the entire mass of data and allow a more detailed analysis of each term to appraise their relevance. It is shown that for low viscosity fluids, the frictional pressure loss is negligible in comparison with the local losses; however, for high viscosity those losses have similar magnitudes.*

Keywords: *Petroleum Engineering, ESP, Artificial Lift, Centrifugal Pumps, Modeling.*

1. INTRODUCTION

An electrical submersible pump (ESP) is a vertical multistage centrifugal pump type with diffuser, which is considered one of the best methods for lift large volumes of liquids. Widely used in the petroleum industry, the ESP is applied to lift oil, pumping in subsea water injection and others. As part of an artificial lift system, ESP is installed in the well in order to increase production.

Recently, oil production increased in wells with high oil viscosity using the ESP system and currently the selection of high performance equipment under such conditions became very significant, having direct impact on oil production.

The flow in a centrifugal pump rarely follows idealized model provided by the Euler equations. Several hydraulic losses can be founded on the literature but the majors' ones are friction losses, shock losses, the first caused by viscous dissipation within the channels of the impeller and diffuser and the second due to misalignment between the streamlines and the blades of the rotors and diffusers.

Pumping of viscous fluids reduces head and also increases the power required by the pump. The power consumption can be idealized as the theoretical power consumption provided by the Euler equations adding the losses associated with the friction between the rotor and the surrounding and power due to hydraulic losses at the end of the rotor is attached to the fact that fluid has a high tangential velocity in this region.

2. LITERATURE REVIEW

For conservation of momentum theorem applied to one-dimensional flow in the rotor, are taken into account only the average velocity on control surfaces. All non-uniformities are ignored.

The resultant moment forces on the blade can be thought of as the integral of the pressure and shear stress on the surface of the blade. If the blade generates a force, this integral is obviously not zero, thereby more pressure on the pressure surface in relation to the suction surface of the blade is expected. (Gulich, 2007).

According Stepanoff (1967), the immediate effect of this pressure profile is the relative velocity of the suction surface is greater than the relative velocity of the pressure surface. The velocity profile is also affected when the flow cannot follow the exact curvature of the blade.

Fraser (1981) carries an interesting discussion of the recirculation occurring in the reduced flows ($Q < Q_{BEP}$), where BEP is best efficiency point, and affirms to be related to the total pressure generated by the pump which is the

sum of the pressure generated by the centripetal force and the dynamic force. The centripetal pressure depends on the diameter and rotation of the rotor, but it is independent of flow rate. The dynamics pressure is a function of the absolute velocity, which is functions of the flow rate.

Gulich (2001) mentions that to strong recirculation, the portion of the flow that recirculates the input is greater than the flow, there is a strong pre-rotation of the flow and the flow enters with wide angle. Thus it is not congruent, causes flow separation and cavitation.

Akhras et. al.(2004) presented detailed results of the flow with a centrifugal pump assembled with diffuser. The measurements were made with Laser Doppler Velocity (LDV) at different operating points. The flow was studied at different positions of the rotor and the diffuser. The specific rotation of the pump used was $\omega_s = 0,577$ with 7 blades and outlet angle is $\beta_2 = 22.5^\circ$. It was observed that for low flow rates the influence of the diffuser is more significant in the rotor leading a significant distortion of the flow causing instabilities and secondary flows.

Feng, Benra, e Dohmen (2009a, 2010 e 2011) investigated, using LDV and Computer Fluid Dynamics (CFD) simulations, the instabilities of the flow field in a radial diffuser pump. It was observed that reducing the flow from the Best Efficiency Point (BEP) the effects of output recirculation increases. The rotation of the rotor causes a periodic inflow condition in the radial direction in the diffuser is considered a source of instability.

There are many authors that propose models to estimate the performance of the pump operating with viscous fluids. The widely model used in industry is that proposed by the Hydraulic Institute, described in ANSI-HI 9.6.7-2010. This correction procedure is based on a large amount of centrifugal pumps experimental data and provides pump performance operating with viscous fluid based on the performance curves with water.

According Monte Verde *et al.* (2013) the comparison of experimental results with the correction method Hydraulic Institute for ESP types showed a good agreement on the head correction factor, being the maximum deviation of around 8%. However, the capacity and efficiency correction factors showed high discrepancy, reaching 45% capacity correction.

Paternost *et al.* (2013) presented a simplified formulation for interpreting the performance curves of centrifugal pumps. The formulation for the one dimensional performance of the pump takes into account the frictional losses and shocks while the formulation for the shaft power consumed takes into account the theoretical power by adding the power consumed by friction with the surrounding fluid and the dissipative effects end of the blades. The model was numerically adjusted to the experimental data obtained in a two-stage centrifugal pump with volute case, presenting itself as a great alternative to the analysis and interpretation of the losses in the flow of viscous fluids in pumps. The present work aims to deepen this formulation, in order to allow a detailed analysis of each loss involved in the flow inside the pump, and validate it by experimental results obtained with real ESP pumps.

3. THEORETICAL MODEL

The equation showed based on Paternost *et al.* (2013) and aims to the interpretation of data characterization for single phase flow in centrifugal pumps. The main contributions of this work are the inclusion of localized losses at the inlet and outlet of the pump as well as a different approach to the power consumed by end effects.

3.1 Dimensional analysis

Dimensional analysis in centrifugal pumps is widely used to better understand the flow and the physical effects involved before starting a theoretical and experimental analysis more extensive, allowing to extract data trends that would otherwise remain disorganized and incoherent.

The output variables Pressure gain (Δp) and shaft power (P_m) are dependent functions on various parameters such as:

$$\begin{aligned} \Delta p &= f_1(Q, D, \omega, \rho, \mu, L_i) \\ P_m &= f_2(Q, D, \omega, \rho, \mu, L_i) \end{aligned} \quad (1)$$

Where Q is volumetric flow rate [m^3/s], D is rotor diameter [m], ω is rotation [1/s], ρ is specific mass [kg/m^3], μ is viscosity [Pa.s] and L_i is generic dimension of pump [m].

The direct application of the concepts of dimensional analysis results in four dimensionless groups defined as:

$$\text{Capacity Coefficient} \rightarrow C_Q = \frac{Q}{\omega D^3} \quad (2)$$

$$\text{Head Coefficient} \rightarrow C_H = \frac{\Delta p}{\rho \omega^2 D^2} \quad (3)$$

$$\text{Power Coefficient} \rightarrow C_P = \frac{P_m}{\rho \omega^3 D^5} \quad (4)$$

$$\text{Viscosity Coefficient} \rightarrow X = \frac{\mu}{\rho \omega D^2} = \frac{1}{Re_\omega} \quad (5)$$

$$\text{Geometry Coefficients} \rightarrow \frac{L_i}{D} \quad (6)$$

So that:

$$\begin{aligned} C_H &= F_1 \left(C_Q, X, \frac{L_i}{D} \right) \\ C_P &= F_2 \left(C_Q, X, \frac{L_i}{D} \right) \end{aligned} \quad (7)$$

The efficiency (η) is already a dimensionless and is only related to the parameters defined in equations (2) (3) and (4):

$$\eta = \frac{C_Q C_H}{C_P} \quad (8)$$

3.2 Analysis of the pressure gain

The performance of the pump can be understood as the pressure gain by Euler deducting the losses:

$$\Delta p = \Delta p_{Euler} - \Delta p_{losses} \quad (9)$$

Where:

$$\Delta p_{Euler} = \rho \omega^2 r_2^2 \left(1 - \frac{q \cot \beta_2}{2\pi b_2 \omega r_2^2} \right) = \frac{1}{4} \rho \omega^2 D^2 - k_1 \left(\frac{L_i}{D} \right) \frac{\rho \omega q}{D} \quad (10)$$

Which $r_2 = \frac{D}{2}$ and k_1 is an explicit function of the pump geometry:

$$k_1 \left(\frac{L_i}{D} \right) = \frac{D \cot \beta_2}{2\pi b_2} \quad (11)$$

The hydraulic losses can be represented by the sum of a friction term and localized losses:

$$\Delta p_{losses} = \Delta p_{friction} + \Delta p_{loc} \quad (12)$$

The friction loss is expressed by an equivalent friction factor, which is composed of one turbulent term (or inertial prevailing in high flow), and a viscous term (which prevails at low flow rates), i.e.:

$$\Delta p_{friction} = f \left(Re, \frac{\epsilon}{D} \right) \frac{L_i \rho}{D} \left(\frac{q}{A_n} \right)^2 = k_2' \left(\frac{L_i}{D} \right) f \left(Re, \frac{\epsilon}{D} \right) \rho \omega^2 D^2 \left(\frac{q}{\omega D^3} \right)^2 \quad (13)$$

Where $A_n = 2\pi \bar{r} \bar{b}$ e:

$$f \left(Re, \frac{\epsilon}{D} \right) = k_3' \left(\frac{L_i}{D} \right) \frac{\mu D}{\rho q} + k_4' \left(\frac{L_i}{D} \right) \left(\frac{\mu D}{\rho q} \right)^n \quad (14)$$

Therefore:

$$\Delta p_{friction} = \left[k_2 \left(\frac{L_i}{D} \right) \frac{\mu D}{\rho q} + k_3 \left(\frac{L_i}{D} \right) \left(\frac{\mu D}{\rho q} \right)^n \right] \rho \omega^2 D^2 \left(\frac{q}{\omega D^3} \right)^2 \quad (15)$$

Which $k_2 = k_2' k_3'$; $k_3 = k_3' k_4'$. The exponent n expresses the viscous effects subsisting at high flow rates and should be considered less than 1. The localized losses are considered purely inertial and independent of viscosity. These losses are represented by the sum of the loss due to impact against the impeller and diffuser as well as those which occur in the inlet and outlet of the pump. The loss by shock is avoid when the pump operates at flow rate $q^* = 2\pi b_1 \omega r_1^2 t \beta_1$. So

$$\Delta P_{loc} = \rho \omega^2 D^2 k_4 \left(\frac{L_i}{D} \right) \left[1 - k_5 \left(\frac{L_i}{D} \right) \frac{q}{\omega D^3} \right]^2 + k_6 \left(\frac{L_i}{D} \right) \rho \omega^2 D^2 \left(\frac{q}{\omega D^3} \right)^2 \quad (16)$$

Where k_5 is an explicit function of the pump geometry:

J. Biazussi, W. Monte Verde, M. Varón, A. Bannwart, V. Estevam.
Comparison of Experimental Curves of ESP with a Simple Single-Phase Approach

$$k_5 \left(\frac{L_i}{D} \right) = \frac{D^3 \cot g \beta_1}{2\pi b_1 r_1^2} \quad (17)$$

Substituting equations (15) and (16) in equation (9) and simplifying the notation of k_i obtained:

$$\Delta p = \frac{1}{4} \rho \omega^2 D^2 - k_1 \frac{\rho \omega q}{D} - \left[k_2 \frac{\mu D}{\rho q} + k_3 \left(\frac{\mu D}{\rho q} \right)^n \right] \rho \omega^2 D^2 \left(\frac{q}{\omega D^3} \right)^2 - \left[\rho \omega^2 D^2 k_4 \left(1 - k_5 \frac{q}{\omega D^3} \right)^2 + k_6 \rho \omega^2 D^2 \left(\frac{q}{\omega D^3} \right)^2 \right] \quad (18)$$

Grouping common terms is obtained:

$$\Delta p = \frac{1}{4} \rho \omega^2 D^2 (1 - 4k_4) - (k_1 - 2k_4 k_5) \frac{\rho \omega q}{D} - k_2 \frac{\mu q}{D^3} - \rho \omega^2 D^2 \left[k_3 \left(\frac{\mu D}{\rho q} \right)^n + k_4 k_5^2 + k_6 \right] \left(\frac{q}{\omega D^3} \right)^2 \quad (19)$$

Note that the viscosity effect disappears when $q = 0$. Dividing by $\rho \omega^2 D^2$ comes to:

$$\frac{\Delta p}{\rho \omega^2 D^2} = \frac{1}{4} (1 - 4k_4) - (k_1 - 2k_4 k_5) \frac{q}{\omega D^3} - k_2 \frac{\mu}{\rho \omega D^2} \frac{q}{\omega D^3} - \left[k_3 \left(\frac{\mu D}{\rho q} \right)^n + k_4 k_5^2 + k_6 \right] \left(\frac{q}{\omega D^3} \right)^2 \quad (20)$$

Or, using the equations (2), (3) and (5):

$$C_H = a_0 - (a_1 + a_2 X) C_Q - \left[a_3 \left(\frac{X}{C_Q} \right)^n + a_4 \right] C_Q^2 \quad (21)$$

Equation (21) is the same obtained by Paternost *et al.* (2013). However, the formulation proposed here in to include localized losses of input and output allows interpretation of different losses separately comparing them with each other and theoretical estimates. To do this, consider the coefficients a_0, a_1, a_2, a_3, a_4 are known from the relations:

$$\begin{aligned} a_0 &= \frac{1}{4} (1 - 4k_4) \\ a_1 &= k_1 - 2k_4 k_5 \\ a_2 &= k_2 \\ a_3 &= k_3 \\ a_4 &= k_4 k_5^2 + k_6 \end{aligned} \quad (22)$$

The relations in Equation (22) allows the determination of coefficients from 6 k_i , remaining one degree of freedom. In principle, one of whose coefficients dependence on geometry is explicit, that is, k_1 or k_5 could be imposed. In this work, we chose to measure directly the coefficient k_1 defined by equation (11) and impose their value to solve the system (22). This choice is justified by the need to establish the theoretical curve of Euler as accurately as possible.

It should be noted that the losses for possible leaks were not included in the analysis, staying as suggestions for future work. It can be concluded that this interpretation of the pressure gain curve of a centrifugal pump requires the simultaneous adjustment of five dimensionless coefficient dependent on the geometry of the pump, and one exponent.

3.3 Analysis of the shaft power

The shaft power is seen as the sum of three parts:

- Hydraulic power $q\Delta P$ transferred to the fluid,
- The power losses caused by the hydraulic fluid in the rotor and diffuser
- The losses associated with the friction between the rotor and the surrounding fluid.

Since the sum of the first two portions is the Euler power, the following dimensional representation for the shaft power can be suggested:

$$\dot{W}_s = q\Delta P_{Euler} + \dot{W}_{Losses} \quad (23)$$

These losses can be considered as the sum of three components, one from mechanical friction, one due to friction disk and the other at the edge of the rotor:

$$\dot{W}_{Losses} = \dot{W}_{mechanical\ friction} + \dot{W}_{disk\ friction} + \dot{W}_{edge} \quad (24)$$

Mechanical power losses are related to the intensity of the axial force, which forces the bearing axle. A formulation of this effect is as follows:

$$\dot{W}_{\text{mechanical friction}} = k_7 \Delta p D^3 \omega \quad (25)$$

where Δp is the pressure gain given by equation (19). The friction disk is regarded as a viscous and inertial contribution:

$$\dot{W}_{\text{disk}} = k_8 \mu \omega^2 D^3 + k_9 \rho \omega^3 D^5 \quad (26)$$

The losses at the end of the rotor are associated with the fact that the fluid has a high tangential velocity in this region. Power dissipation to be expected either due to contact with the rotating fluid shell as with the entry of the diffuser (blink alignment of the rotor blades at the exit to the entrance of the diffuser). The tangential velocity component at the tip of the rotor is given by:

$$V_{t2} = \omega r_2 - \frac{q \cot \beta_2}{2\pi r_2 b_2} = \omega D \left(\frac{1}{2} - \frac{2k_1 q}{\omega D^3} \right) \quad (27)$$

The following expression, given inertial and viscous contributions can be suggested to express the dissipative effects at the edge of the rotor:

$$\dot{W}_{\text{edge}} = k'_{10} \mu \frac{V_{t2}^2}{D} A_{n2} + k'_{11} \rho V_{t2}^3 A_{n2} = k'_{10} \rho V_{t2}^2 A_{n2} \left(\frac{\mu}{\rho D} + \frac{k'_{11}}{k'_{10}} V_{t2} \right) \quad (28)$$

Substituting equation (26) in equation (27), developing and making the relevant simplification is obtained:

$$\dot{W}_{\text{edge}} = k_{10} \rho \omega^3 D^5 \left(\frac{1}{2} - \frac{2k_1 q}{\omega D^3} \right)^2 \left[\frac{\mu}{\rho \omega D^2} + k_{11} \left(\frac{1}{2} - \frac{2k_1 q}{\omega D^3} \right) \right] \quad (29)$$

Assembling the above results in a single expression yields the following result:

$$\begin{aligned} \dot{W}_s = & q \left(\frac{1}{4} D^2 \rho \omega^2 - \frac{q \rho \omega k_1}{D} \right) + D^3 \Delta p \omega k_7 + D^3 \mu \omega^2 k_8 \\ & + D^5 \rho \omega^3 k_9 + D^5 \rho \omega^3 \left(\frac{1}{2} - \frac{2q k_1}{D^3 \omega} \right)^2 k_{10} \left(\frac{\mu}{D^2 \rho \omega} + k_{11} \left(\frac{1}{2} - \frac{2q k_1}{D^3 \omega} \right) \right) \end{aligned} \quad (30)$$

Dividing by $\rho \omega^3 D^5$:

$$\begin{aligned} \dot{W}_s = & \frac{q}{4D^3 \omega} - \frac{q^2 k_1}{D^6 \omega^2} + \frac{\Delta p k_7}{D^2 \rho \omega^2} + \frac{\mu k_8}{D^2 \rho \omega} + k_9 + \frac{\mu k_{10}}{4D^2 \rho \omega} + \frac{1}{4} k_{10} k_{11} \left(\frac{1}{2} - \frac{2q k_1}{D^3 \omega} \right) \\ & + \frac{q \left(-\frac{2\mu k_1 k_{10}}{D^2 \rho \omega} - 2k_1 k_{10} k_{11} \left(\frac{1}{2} - \frac{2q k_1}{D^3 \omega} \right) \right)}{D^3 \omega} + \frac{q^2 \left(\frac{4\mu k_1^2 k_{10}}{D^2 \rho \omega} + 4k_1^2 k_{10} k_{11} \left(\frac{1}{2} - \frac{2q k_1}{D^3 \omega} \right) \right)}{D^6 \omega^2} \end{aligned} \quad (31)$$

Developing and grouping the common terms, one reaches:

$$\begin{aligned} C_P = & \left(\frac{k_{10} k_{11}}{8} + k_9 \right) + \left(\frac{k_{10}}{4} + k_8 \right) X + C_H k_7 + C_Q \left(\left(\frac{1}{4} - \frac{3}{2} k_1 k_{10} k_{11} \right) - 2k_1 k_{10} X \right) \\ & + C_Q^2 \left((-k_1 + 6k_1^2 k_{10} k_{11}) + 4k_1^2 k_{10} X \right) - (8k_1^3 k_{10} k_{11}) C_Q^3 \end{aligned} \quad (32)$$

Using the dimensionless definitions showed equations (2), (3) and (5):

$$C_P = b_0 + b_1 X + b_2 C_H + (b_3 - b_4 X) C_Q + (b_5 + b_6 X) C_Q^2 - b_7 C_Q^3 \quad (33)$$

Where:

J. Biazussi, W. Monte Verde, M. Varón, A. Bannwart, V. Estevam.
Comparison of Experimental Curves of ESP with a Simple Single-Phase Approach

$$\begin{aligned}
 b_0 &= \frac{k_{10}k_{11}}{8} + k_9 \\
 b_1 &= k_8 + \frac{k_{10}}{4} \\
 b_2 &= k_7 \\
 b_3 &= \frac{1}{4} - \frac{3}{2}k_1k_{10}k_{11} \\
 b_4 &= 2k_1k_{10} \\
 b_5 &= -k_1 + 6k_1^2k_{10}k_{11} \\
 b_6 &= 4k_1^2k_{10} \\
 b_7 &= 8k_1^3k_{10}k_{11}
 \end{aligned} \tag{34}$$

The same as the pressure gain, we assume that the constant k_1 known. It can be concluded that this interpretation of shaft power curve for centrifugal pump requires the simultaneous adjustment of five dimensionless coefficient dependent on the geometry of the pump.

4. TEST FACILITIES AND PROCEDURE

Aim in to investigate the ESP's performance operating with viscous liquid flow, an experimental test loop was assembled. The experimental facilities were assembled at LABPETRO, a laboratory from the "Petroleum Studies Center" (Cepetro-UNICAMP).

The ESP's test loop is schematically illustrated in Fig. 1. This circuit consists of a conventional ESP driven by a three phase induction motor 380 V, 50 hp, controlled by a frequency inverter. A booster pumps water from the reservoirs to the test line. By controlling the frequency of its motor, the booster's main function is to control pressure at the entrance of the ESP. The liquid mass flow is obtained by a Coriolis meter located at the suction line of the ESP. After being pumped by the ESP, the liquid returns to the tanks. Pressure, temperature, viscosity, torque on the drive shaft of the ESP, flow rate and voltage on the electric motor are also measured in the test. The variables measured in the test are conditioned by voltage (0-10V) or current (4-20mA) modules.

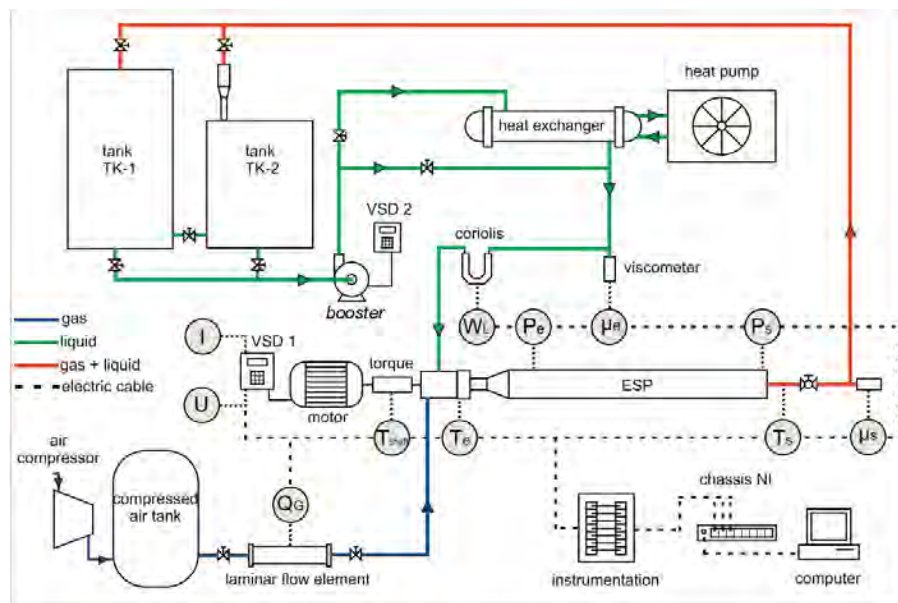


Figure 1 – ESP bench test, located at State University of Campinas, São Paulo/Brazil.

A supervisory system dedicated to loop processes and presents this operational data and performance results through a friendly interface.

In the program the user can operate the data acquisition sampling rate and the number of desired samples. In addition, each experimental point recorded is immediately drawn on a graph that allows you to observe the quality of the data being obtained (elevation and efficiency as a function of flow) in real time. In Fig. 2 it can be seen the interface.

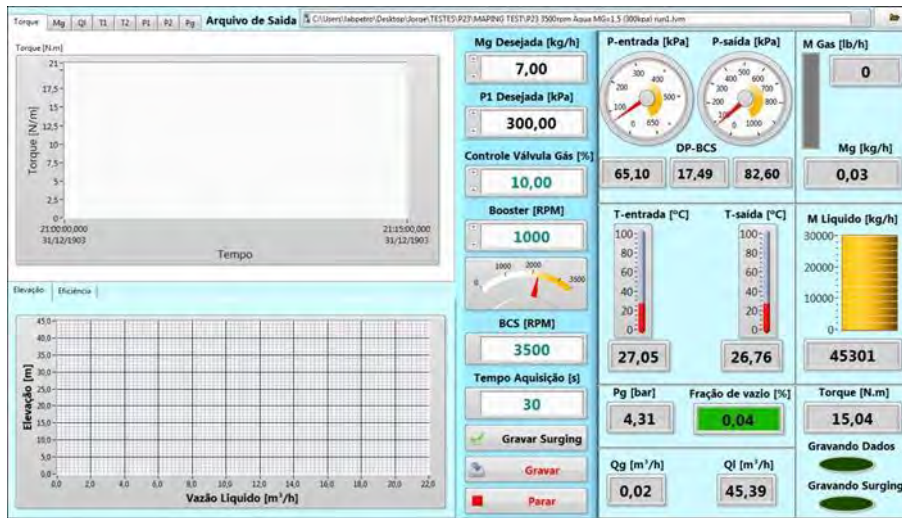


Figure 2 – Program interface for control and data acquisition.

4.1 Pump P47 Series 538

The pump P47 is constructed with three stages, each stage consisting of an impeller and a diffuser, as shown in Fig. 3. For this model. The manufacturer gives the following characteristics operating at 3500rpm with water:

- Shut-off $\approx 21\text{m}$;
- Open flow $\approx 54,18\text{ m}^3/\text{h}$;
- Head on BEP $\approx 15,85\text{m}$;
- Flow rate on BEP $\approx 31,46\text{ m}^3/\text{h}$;
- Efficiency on BEP $\approx 65\%$
- External diameter Rotor (D) 108 mm
- Output channel height (b_2) 7mm
- Output Angle (β_2) $22,8^\circ$



Figure 3 – Pump impeller and diffuser P47 series 538.

To obtain the constants of the model were performed an experimental program in order to acquire the performance curve of the ESP for rotations 2400 and 3500rpm and viscosities of 1, 23, 33, 40, 46, 77, 120 and 180cP. The viscosity of 1cp used water as the working fluid and other viscosities were achieved using mineral oil and controlling the temperature to reach the desired points

5. RESULTS AND DISCUSSIONS

First, we present the experimental results of the ESP operating with viscous fluid. Posteriorly shows the fit of the model with experimental data and finally it was conduct a discussion about the losses and their behavior depending on the viscosity.

J. Biazussi, W. Monte Verde, M. Varón, A. Bannwart, V. Estevam.
 Comparison of Experimental Curves of ESP with a Simple Single-Phase Approach

5.1 Experimentals Results

The manufacturer's curves of performance and efficiency for one stage are shown in Fig. 4 and compared with the experimental results. It is observed to performance curve, the data points are in accordance with the manufacturer, but for the efficiency curves the manufacturer shows values slightly higher than those recorded in tests.

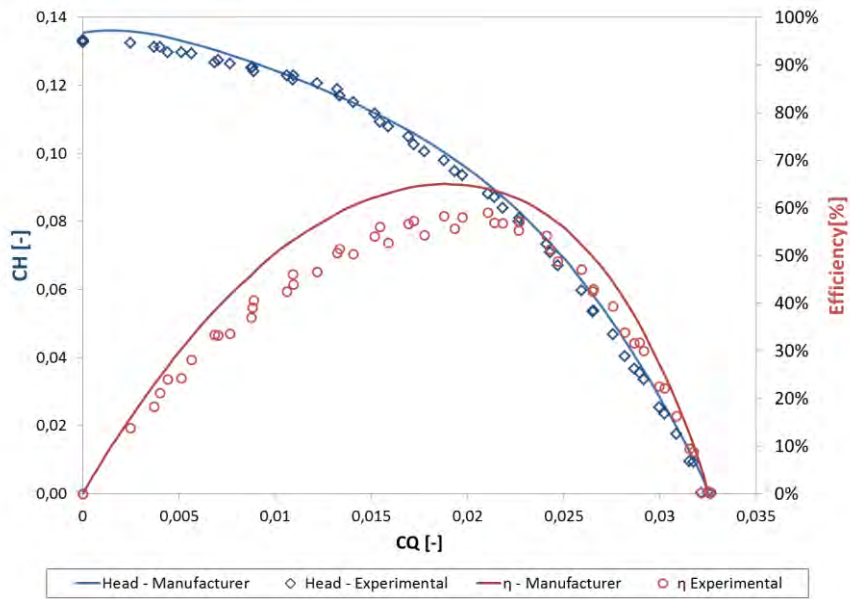


Figure 4 - Manufacturer curves of performance and efficiency pump P47 series 538.

In the Figure (5) and (6) are shown the results of the ESP performance curve operating at 2400rpm and 3500rpm respectively, with different viscosities.

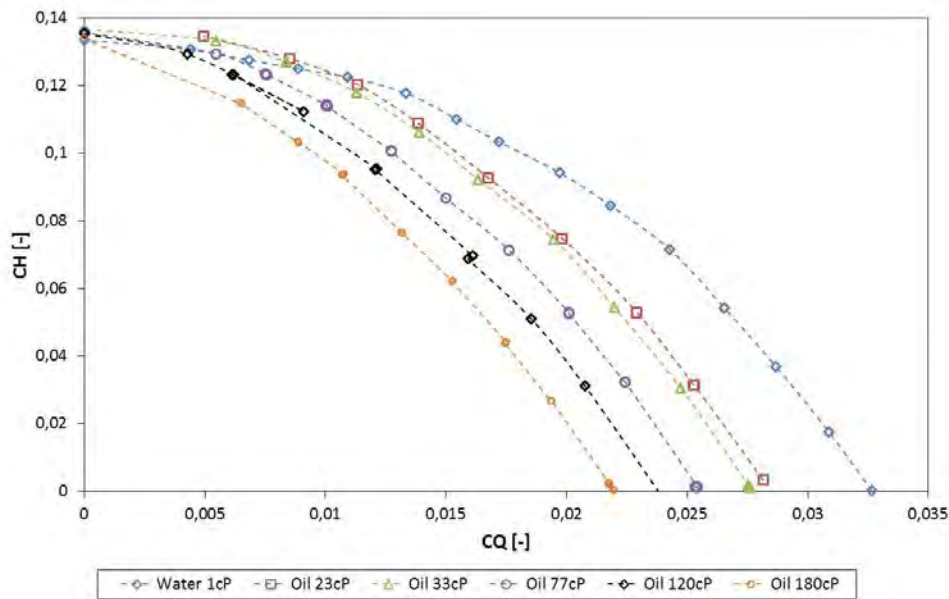


Figure 5 – ESP performance curves for P47 running at 2400rpm.

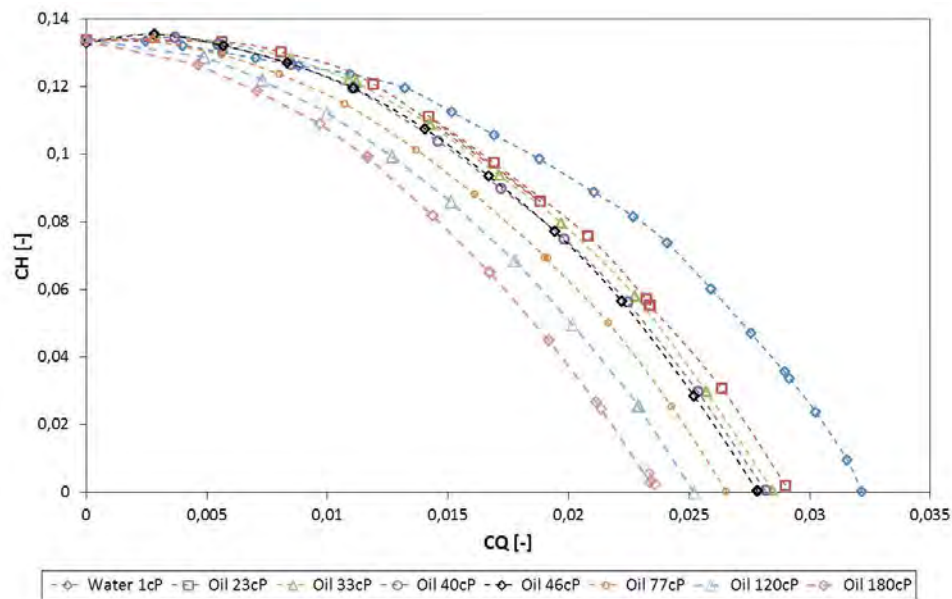


Figure 6 – ESP performance curves for P47 running at 3500rpm.

The best efficiency point is changed when the pump works with different viscosity fluids. This change can be observed experimentally in efficiency curves, as shown in Fig. 7.

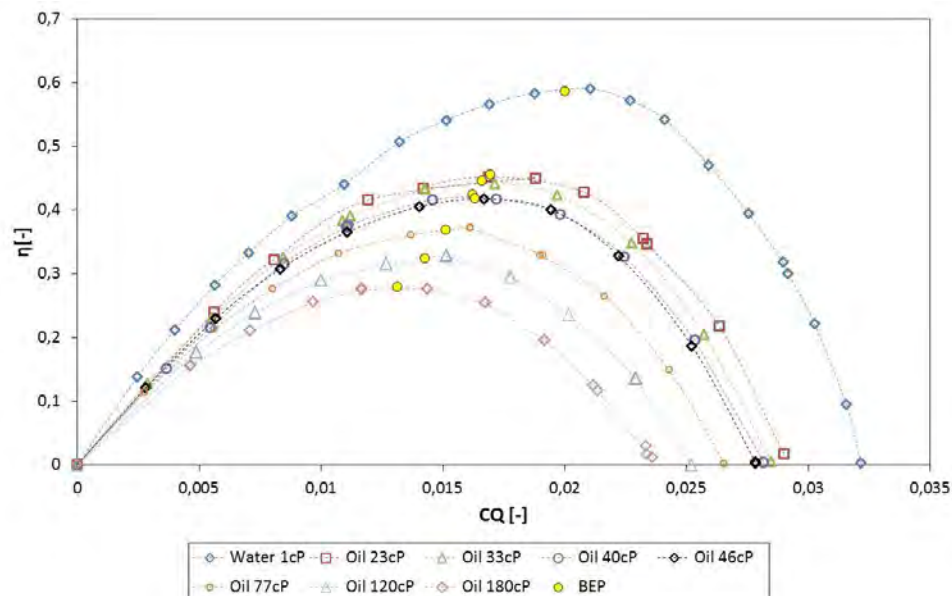


Figure 7 – Efficiency curves for ESP operating at 3500rpm.

5.2 Model Results

To obtain the constants of the model we used software Mathematica ® 8.0 by Wolfram. For equations (21) and (33) constants that best represent the experimental points are shown in Table 1. The dimensionless geometric constant defined in Equation (11) for this pump is $k_1 = 5,8415$.

In Fig. (8) It is shown that the experimental points obtained were in good agreement with the calculated points with the model presented deviate by less than 10%.

Fig. (9) shows the comparison of calculated data with the experimental data for shaft power. It is found that the dispersion of the points was larger than the dispersion points of the head curve, but still showed a good fit, it is considered that greater dispersion due to larger uncertainty in the measurement of torque.

J. Biazussi, W. Monte Verde, M. Varón, A. Bannwart, V. Estevam.
Comparison of Experimental Curves of ESP with a Simple Single-Phase Approach

Table 1 – Constant adjusted with experimental data for the proposed model.

Equation 21		Equation 33	
a_0	0,13276	b_0	0,00241
a_1	-1,49981	b_1	25,18292
a_2	35885,9	b_2	0
a_3	267,5133	b_3	0,10077
a_4	119,9373	b_4	0,18641
n	0,14541	b_5	-2,35474
		b_6	2,17790
		b_7	27,15699

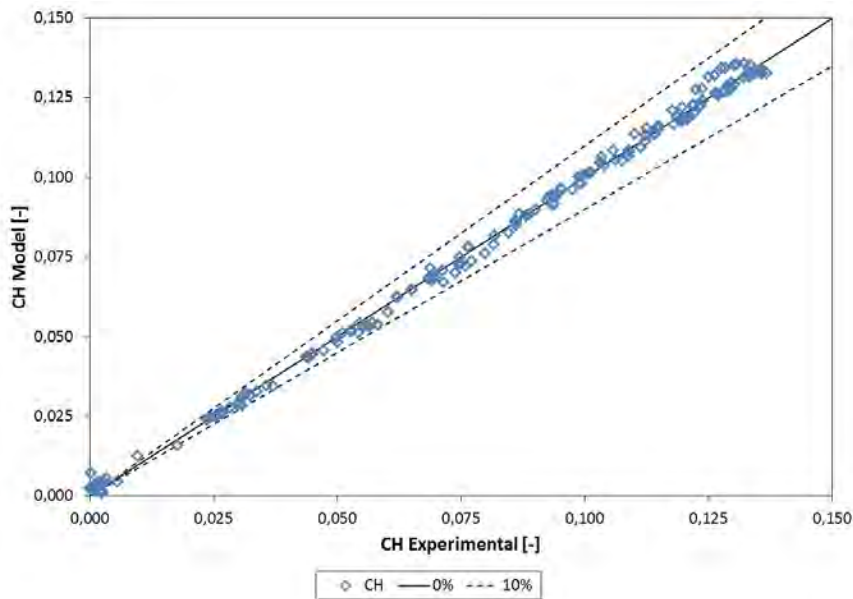


Figure 8 – Comparison of the calculated data with the experimental data for pressure gain.

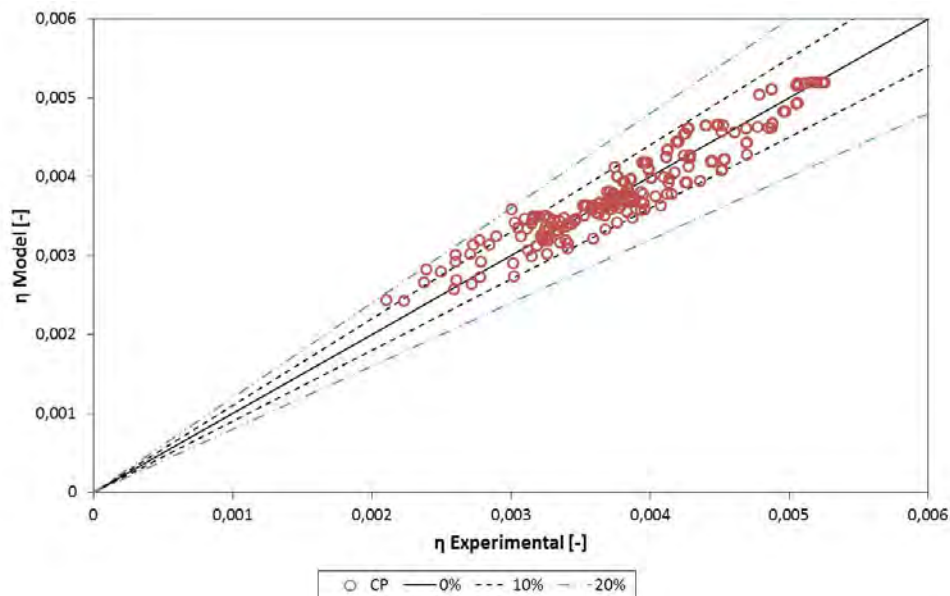


Figure 9 – Comparison of the calculated data with the experimental data for shaft power.

Through Equations (8), (21) and (33) is possible to calculate the efficiency of the model. The values presented by the models were compared with the experimental data collected and presented in Fig. 10. Even with the propagation of

errors of two equations, the efficiency was in agreement with experimental data. The most parts of the model points remain in a range of $\pm 10\%$ compared with the experimental data.

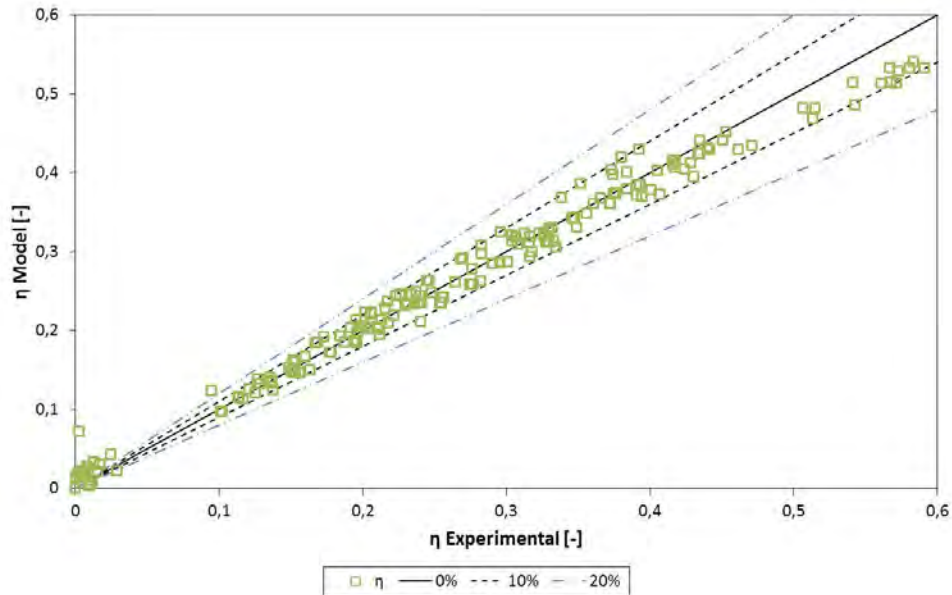


Figure 10 – Comparison of the calculated data with the experimental data for efficiency.

In Fig. (11) are shown the experimental points pumping water operating at 2400 rpm and 3500 rpm. It is verify that the model does not show different significantly for the rotations tested indicating that the flow regime is turbulent and the friction factor is less sensitive to increased flow.

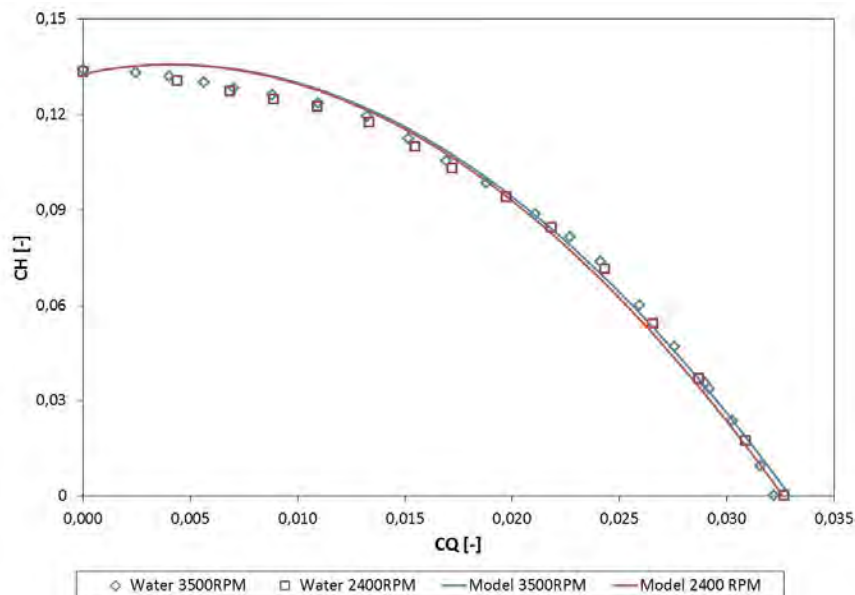


Figure 11 – Comparison of experimental points with the model curve for 1cP and rotations 2400 and 3500rpm.

However, in Fig. 12, which shows the comparison of the experimental data with the model to oil with 180cP of viscosity and 2400 rpm and 3500rpm, it is observed that the dimensionless performance changes with pump speed. This is explained by increased friction factor when the pump operates at lower Reynolds, thereby increasing the viscous flow losses within the rotor.

J. Biazussi, W. Monte Verde, M. Varón, A. Bannwart, V. Estevam.
Comparison of Experimental Curves of ESP with a Simple Single-Phase Approach

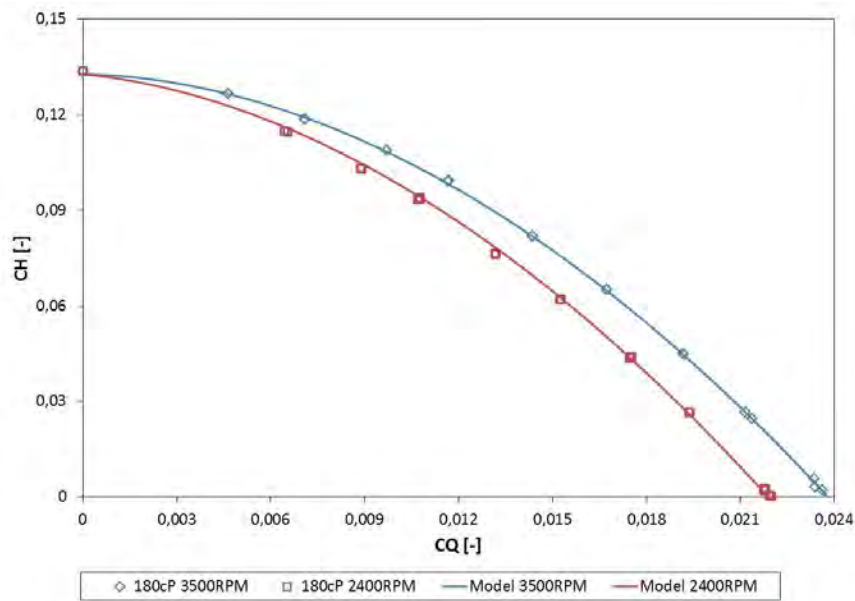


Figure 12 – Comparison of experimental points with the model curve for 180cP and rotations 2400 and 3500rpm.

5.3 Discussions about the losses in the performance curve

In this section it was discussed the behavior of the losses represented by the model.

In Fig. (13) is shown the performance model curve and their portions. The idealized pressure gain (blue line) discounted losses result in effective performance curve (black line) of the pump. It is seen that the localized losses depending on flow rate indicating a point of minimum. This minimum point of localized losses can be understood as a point where the shock losses at the entrance and exit of the rotors and diffusers are minimized. Already friction loss for a fluid of low viscosity represents a very small portion of the losses.

The curve CH_{Losses} represents the sum of hydraulic losses. It is important to note that the minimum point of localized losses is not of the same point of the sum of the hydraulic losses and is also different from the best efficiency point.

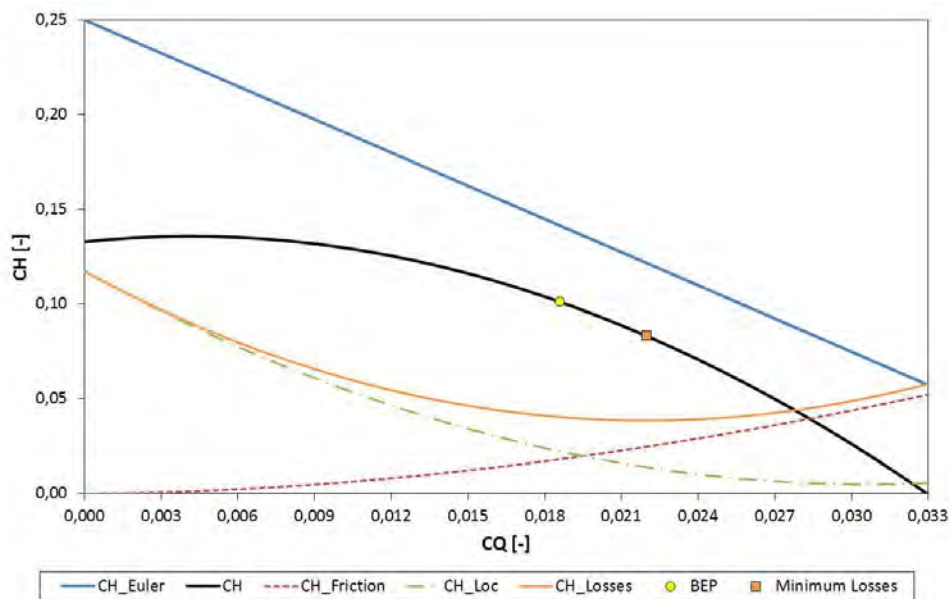


Figure 13 – Losses model representation for the 3500rpm 1cP.

In Fig. (14) it is observed that for a fluid with high viscosity, friction losses increase and the effective performance curve has large deviates from the ideal behavior. The localized losses was independent of viscosity than it's not change from the previous figure, but the point of minimum in the sum of the hydraulic losses and BEP is changed.

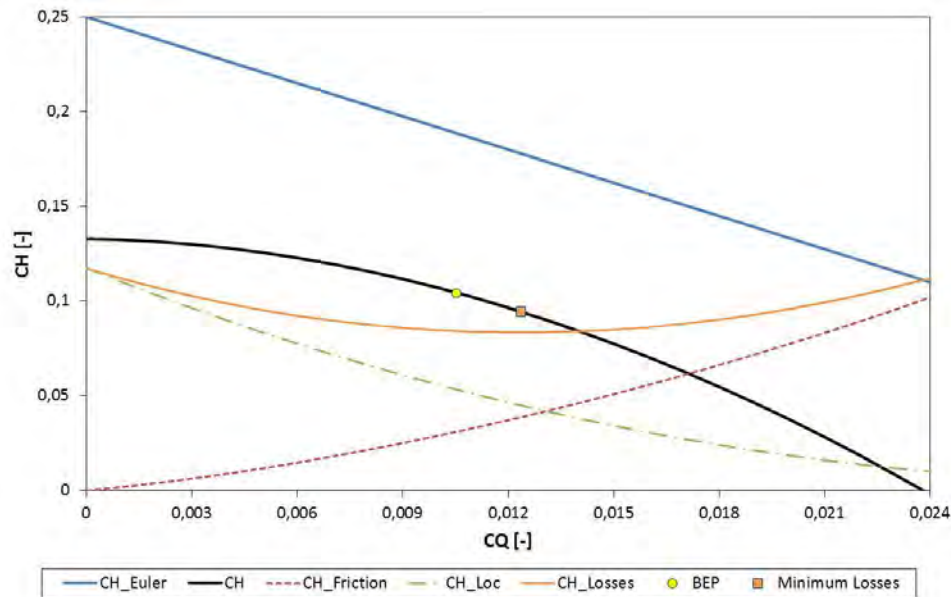


Figure 14 – Representação do modelo e das perdas para 180cP a 3500RPM.

Figure 15 presents the losses for three of different viscosity points. It is possible to observe that the localized losses are independent of viscosity, but the friction losses increase with the viscosity and flow rate. The same behavior is observed for rotations 2400rpm, but the losses are slightly larger, it was expected due to the dependence on Reynolds with rotation.

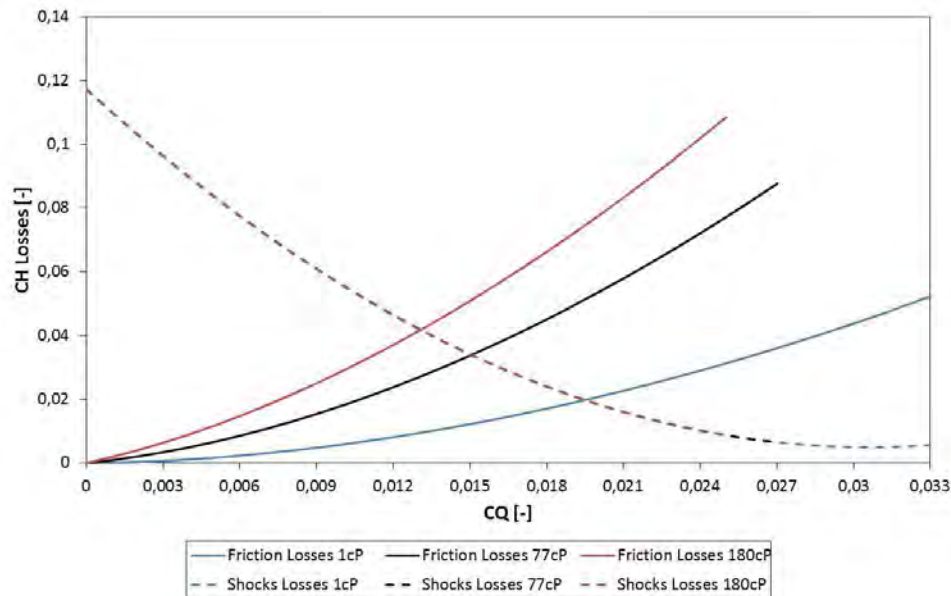


Figure 15 – Portion of losses represented by the model for three viscosities at 3500rpm.

5.4 Discussion of the portion in the shaft power curves

The idealized model for this work has four main power components. The power supplied to the fluid, represented by Euler power (net power add hydraulic losses), disk power (inertial and viscous component), the mechanical power (mechanical friction proportional to the axial force) and the power dissipated by the effects of vortices at the edge of the rotor blades. The sum of all components results in the overall power required by the pump.

According to the fit model obtained, the constant B_2 that multiplies mechanical power was equal to zero, eliminating the term of mechanical power. As the bearings and pump used are new, these terms of losses showed irrelevant, but in other systems or pumps this term may be relevant.

In Fig. (16) it is observed that for low viscosity fluids such as water, a component referring to the friction disk is very small and less than the amount consumed by the edge vortices. This loss was considered consistent, it decreases when the agreement of streamlines with the geometry improves, but does not become zero. This behavior is also expected because power consumption due to the intermittency of the rotor blades and the diffuser generates a power loss. CP_Losses curve represents the sum of all power losses, and its minimum point as the best efficiency point.

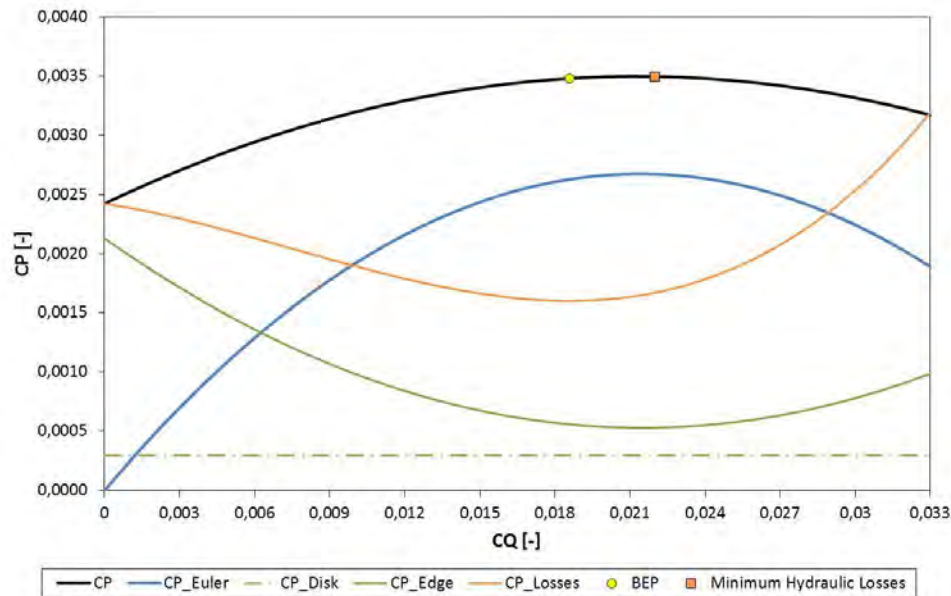


Figure 16 – Portions of the shaft power consumption represented by the model for 1CP operating at 3500rpm.

However in Fig (17), which shows the portions behavior of shaft the power consumed for fluid 180cP operating at 3500rpm, it appears that the portion of the disk friction increases considerably with the viscosity impacting directly whit the total power consumed.

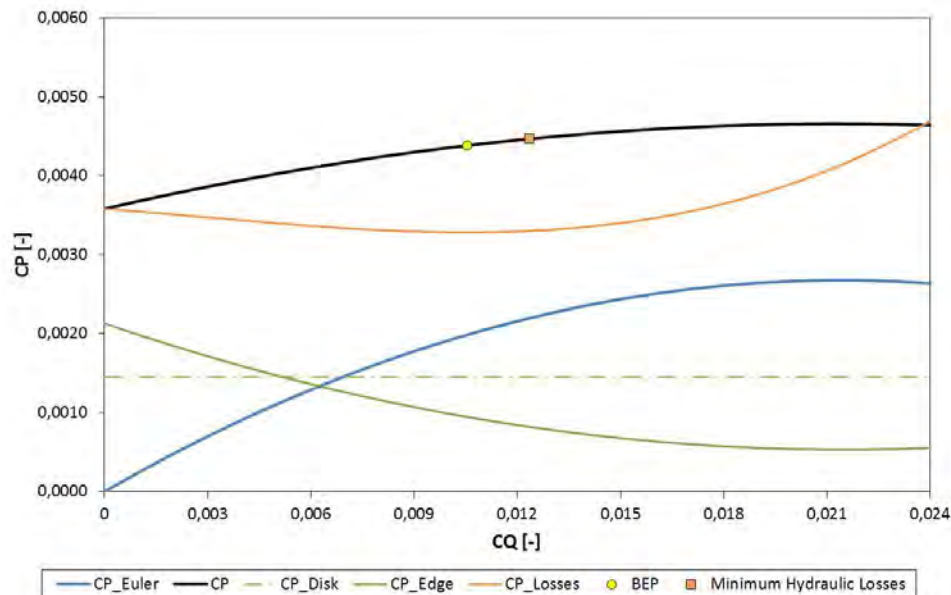


Figure 17 – Portions of the shaft power consumption represented by the model for 180cP operating at 3500rpm.

Fig. (18) and (19) are shown only portions of shaft power consumption that does not generate useful power to fluid in rotation 2400 and 3500 rpm respectively. According to the simplified model have been two installments for the direct consumption of shaft power and one portion related to hydraulic losses. The portion relating to the friction disk has a shaft power consumption independent of the flow rate, and increases significantly with increasing viscosity (dash dot line). The shaft power consumption for edge effects is presented as one of the largest portions in power consumption

and independent of viscosity (solid line). Hydraulic losses and therefore respectively shaft power consumption shown strongly dependent on viscosity and flow rate corresponding to a significant portion of the power consumed by the pump that generates no useful work (dashed line). For the rotation of 3500 rpm it was observed losses behavior like 2400rpm, but slightly smaller.

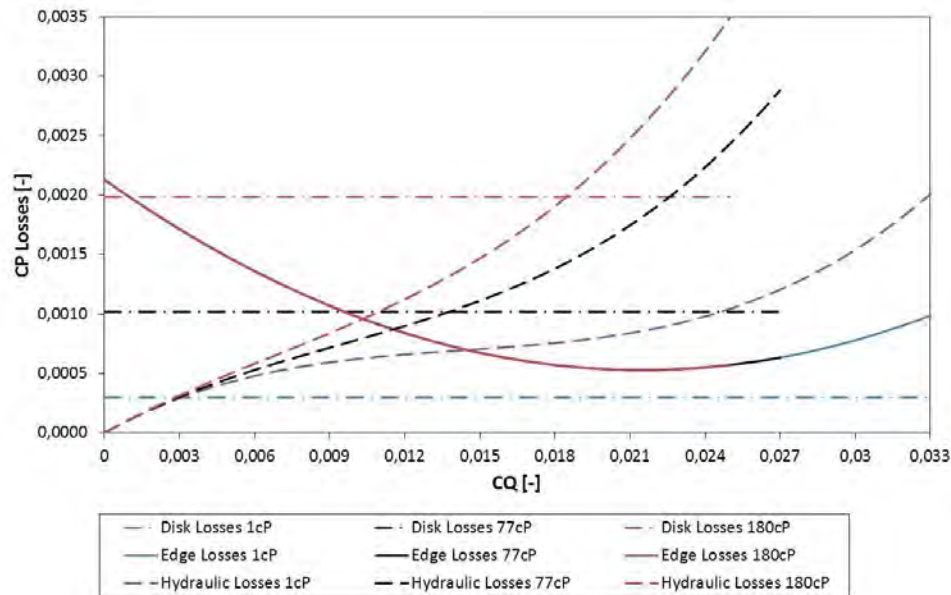


Figure 18 – Portion of shaft power consumption represented by the model for three viscosities at 2400rpm.

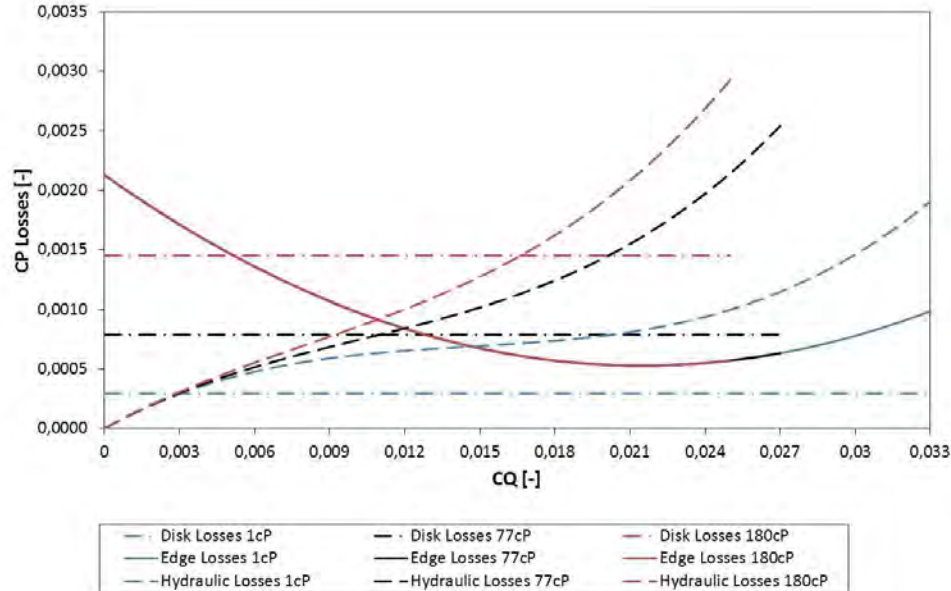


Figure 19 – Portion of shaft power consumption represented by the model for three viscosities at 3500rpm.

6. CONCLUSIONS

Considering the Euler's equation and theoretical losses in the pump, along with experimental data, it was possible to obtain equations that can represent, with good agreement, the head, break horsepower and efficiency of the pump as a function of the capacity coefficient and the Reynolds number. The model allows consistent interpretation of the losses in the performance and shaft power curve.

Both, the model and the experimental data show a severe degradation of performance of the pump as a function of viscosity. When viscosity increase pump performance becomes a function of the Reynolds consequently the rotation, this effect is neglected in the classical theory of one-dimensional pumps.

J. Biazussi, W. Monte Verde, M. Varón, A. Bannwart, V. Estevam.
Comparison of Experimental Curves of ESP with a Simple Single-Phase Approach

It is observed that the best efficiency point does not match the minimum hydraulic losses point. The best efficiency point takes into account all power losses, so this point is not necessarily the point which the fluid will have the smallest losses by shock.

7. ACKNOWLEDGEMENTS

The authors would like to thank PRH and Petrobras for the financial support.

8. REFERENCES

- FENG, Jianjun; BENRA, F.-K.; DOHMEN, H. J. Comparison of periodic flow fields in a radial pump among CFD, PIV, and LDV results. *International Journal of Rotating Machinery*, v. 2009, 2009 a.
- FENG, J.; BENRA, F. K.; DOHMEN, H. J. Investigation of turbulence and blade orientation effects in a radial diffuser pump by laser Doppler velocimetry. *Proceedings of the Institution of Mechanical Engineers, Part A: Journal of Power and Energy*, v. 223, n. 8, p. 991-999, 2009 b.
- FENG, J.; BENRA, F. K.; DOHMEN, H. J. Unsteady flow investigation in rotor-stator interface of a radial diffuser pump. *Forschung im Ingenieurwesen*, v. 74, n. 4, p. 233-242, 2010.
- FENG, JIANIUN; BENRA, Friedrich-Karl; DOHMEN, Hans Josef. Investigation of periodically unsteady flow in a radial pump by CFD simulations and LDV measurements. *Journal of turbomachinery*, v. 133, n. 1, 2011.
- FRASER, Warren H. Flow recirculation in centrifugal pumps. In: ASME meeting. 1981.
- GÜLICH, J. F. Selection criteria for suction impellers of centrifugal pumps. *World Pumps*, v. 2001, n. 414, p. 29-32, 2001.
- GÜLICH, Johann Friedrich. *Centrifugal pumps*. Springer, 2007.
- MONTE VERDE, William. *Estudo experimental de bombas de BCS operando com escoamento bifásico gás-liquido*. 2011.
- MONTE VERDE, William et al. Gas and Viscous Effects on the ESPs Performance. In: 2013 SPE Artificial Lift Conference-Americas. 2013.
- PATERNOST, Guilherme; BANNWART, Antonio; ESTEVAM, Valdir. Experimental Study of Centrifugal Pump Handling Viscous Fluid and Two-Phase Flow. In: 2013 SPE Artificial Lift Conference-Americas. 2013.
- VARON, Mauricio Pardo. Study of an Electrical Submersible Pump (ESP) as Flow Meter. In: 2013 SPE Artificial Lift Conference-Americas. 2013.

9. RESPONSIBILITY NOTICE

The author(s) is (are) the only responsible for the printed material included in this paper.